ORIGINAL RESEARCH

Preparation and biodistribution of [188]Re-labeled folate conjugated human serum albumin magnetic cisplatin nanoparticles ([188]Re-folate-CDDP/HSA MNPs) in vivo

Qiu-Sha Tang[1,*]
Dao-Zhen Chen[2,*]
Wen-Qun Xue[2]
Jing-Ying Xiang[2]
Yong-Chi Gong[1]
Li Zhang[2]
Cai-Qin Guo[2]

[1]Department of Pathology and Pathophysiology, Medical College, Southeast University, Nanjing, Jiangsu; [2]Central Laboratory, Wuxi Hospital for Maternal and Child Health Care, Affiliated Medical School of Nanjin, Wuxi, Jiangsu, China

*Authors contributed equally to this work

Background: The purpose of this study was to develop intraperitoneal hyperthermic therapy based on magnetic fluid hyperthermia, nanoparticle-wrapped cisplatin chemotherapy, and magnetic particles of albumin. In addition, to combine the multiple-killing effects of hyperthermal targeting therapy, chemotherapy, and radiotherapy, the albumin-nanoparticle surfaces were linked with radionuclide [188]Re-labeled folic acid ligand ([188]Re-folate-CDDP/HSA).

Methods: Human serum albumin was labeled with [188]Re using the pre-tin method. Reaction time and optimal conditions of labeling were investigated. The particles were intravenously injected into mice, which were sacrificed at different time points. Radioactivity per gram of tissue of percent injected dose (% ID/g) was measured in vital organs. The biodistribution of [188]Re-folate-CDDP/HAS magnetic nanoparticles was assessed.

Results: Optimal conditions for [188]Re-labeled folate-conjugated albumin combined with cisplatin magnetic nanoparticles were: 0.1 mL of sodium gluconate solution (0.3 mol/L), 0.1 mL of concentrated hydrochloric acid with dissolved stannous chloride (10 mg/mL), 0.04 mL of acetic acid buffer solution (pH 5, 0.2 mol/L), 30 mg of folate-conjugated albumin combined with cisplatin magnetic nanoparticles, and $^{188}ReO_4$ eluent (0.1 mL). The rate of [188]Re-folate-CDDP-HSA magnetic nanoparticle formation exceeded 90%, and radiochemical purity exceeded 95%. The overall labeling rate was 83% in calf serum at 37°C. The major uptake tissues were the liver, kidney, intestine, and tumor after the [188]Re-folate-CDDP/HSA magnetic nanoparticles were injected into nude mice. Uptake of [188]Re-folate-CDDP/HSA magnetic nanoparticles increased gradually after injection, peaked at 8 hours with a value of 8.83 ± 1.71, and slowly decreased over 24 hours in vivo.

Conclusion: These results indicate that [188]Re-folate-CDDP/HSA magnetic nanoparticles can be used in radionuclide-targeted cancer therapy. Surface-modified albumin nanoparticles with folic acid ligand-labeled radionuclide ([188]Re) were successfully prepared, laying the foundation for a triple-killing effect of thermotherapy, chemotherapy, and radiation therapy.

Keywords: cisplatin, folic acid, albumin, magnetic nanoparticles, [188]Re, ovarian cancer

Introduction

Among the most common malignancies of the female reproductive organs, ovarian cancer occurs with the third highest incidence, second only to cervical and uterine carcinomas. However, ovarian cancer is the leading cause of death associated with gynecological malignancy. It is difficult to identify tissue types, and their benign or malignant nature, owing to the complexity of ovarian tissue, despite the ovary being

Correspondence: Qiu-Sha Tang
Medical College, Southeast University,
Nanjing 210009, China
Tel +86 25 8327 2373
Fax +86 25 8327 2373
Email panyixi-tqs@163.com

3077

small in size. About 30% of ovarian cancers are found at an early stage, often during exploratory laparotomy and in the absence of overt symptoms. However, most (70%) of these tumors are at an end stage when first diagnosed, with metastasis to the uterus, annexes, greater omentum, and various organs in the pelvic cavity. Therefore, most patients miss their chance to get early treatment. Current treatment for ovarian cancer is mainly surgery in conjunction with chemotherapy and radiotherapy. End-stage ovarian cancer often recurs after treatment, and is extremely hard to treat. As a result, the 5-year survival rate is as low as 20%–30%.[1] Therefore, development of new therapeutic drugs and strategies has practical relevance.

Thermotherapy is a method of treating tumor tissue using heat generated by various physical energies in human tissues to raise and maintain a cell temperature higher than 40°C for a period of time sufficient to kill cancer cells while avoiding damage to normal cells. During the past 20 years, with the developments in biology, physics, and medical technology, both the theories and techniques of thermotherapy have been advanced rapidly. Among the various heating methods that have been developed, microwave, radiofrequency, and ultrasonic waves are standard methods with obvious therapeutic effects in both superficial and luminal tumors. However, due to partial reflection of electromagnetic waves by the body contour and the electric properties of human tissue, it is difficult for the energy of electromagnetic waves to concentrate in the deep tumor layers. This may cause nonuniform heat distribution.[2,3] In addition, it is hard to measure and maintain a constant temperature accurately at the deeper layers, which also limits the application of thermotherapy in the treatment of cancer.

Usually metastasizing via local spread and abdominal seeding, ovarian cancer is thermosensitive. It tends to localize in the abdominal cavity, even at end stage, and thus is suitable for treatment with intraperitoneal chemohyperthermia. This technique was first used in the clinic by Spratt et al in 1980. The strategy is to combine high temperature and chemotherapy to eliminate free cancer cells and small residual cancerous lesions in the abdominal cavity in order to prevent or reduce local postoperative recurrence and metastasis. Recently, intraperitoneal chemohyperthermia has attracted further attention and been widely used throughout the world, achieving satisfactory therapeutic outcomes.[4–6] The National Cancer Research Institute in Italy has carried out stage II testing of intraperitoneal chemohyperthermia (cisplatin + mitomycin C) in 27 cases of recurrent ovarian cancer, and the two-year survival rate was 55%, with a median

time to local tumor progression of 21.8 months. Of note, a stage III study of 415 patients with end-stage ovarian cancer showed that the median survival time in patients treated with combined chemotherapy via the venous and abdominal cavity routes was 65.6 months, while that of patients who received only intravenous chemotherapy was 49.7 months.[7] The results of this study were considered to represent major progress in clinical gynecological oncology in 2006 by the American Society of Clinical Oncology. The US National Cancer Research Institute has also made a statement recommending that such patients should be treated with chemotherapy delivered by both the venous and abdominal cavity routes. However, because intraperitoneal chemohyperthermia is an invasive method, and both targeted chemotherapy and thermotherapy have some disadvantages, adverse effects are inevitable. In addition, many complications have occurred when intraperitoneal chemohyperthermia has been used clinically, including intestinal obstruction,[8] anastomotic leakage[8,9] renal damage,[9] and bone marrow inhibition,[10,11] which has limited the wider clinical application of this technology. The National Surgical Adjuvant Breast and Bowel Project and American College of Surgeons Oncology Group have organized several research programs to address some of the fundamental problems of intraperitoneal chemohyperthermia, in particular to improve the heating equipment and methods used to measure and maintain deep layer temperature accurately, to increase the effective target orientation, and decrease the side effects of chemotherapy.

The concept of magnetic targeted chemotherapy was proposed by Gilchrist et al in 1957.[11] Magnetic materials in the circulation can not only reach the target[13] precisely under the influence of an applied static magnetic field but can also absorb electromagnetic wave energy and generate heat to control and maintain temperature within the required range (42°C–46°C) for a period of time sufficient to destroy cancer tissue and avoid damage to normal tissues outside the target area under the alternative magnetic field. A novel nanotechnology method combined with thermotherapy was used by Jordan et al in Germany[14–16] to treat tumor tissue, which was a major step forward. Fluid containing magnetic nanoparticles was injected into the transplanted tumors of breast cancer-bearing C_3H mice. When locally radiated in an alternative magnetic field, the magnetic particles absorbed energy and the temperature rose to 47°C. As a result, the tumor was controlled effectively. This new method is called magnetic fluid heating. Acted on by an alternative magnetic field, the magnetic nanoparticles can absorb more energy and generate more heat than microparticles, leading to a better

thermotherapeutic effect and a more uniform increase in temperature. Jordan et al also found that the ability of tumor cells to absorb ferrous nanoparticles is 8–400 times that of normal cells, and that the tumor cells still contained magnetic nanoparticles during division. Quantitative analysis by electron microscopy showed that descendant cells contained on average 50% of the magnetic nanoparticles contained by the parent cells. Tumor cells containing these magnetic nanoparticles can be destroyed easily by magnetic fluid heating. According to the literature, magnetic fluid heating has several important characteristics.[17] First, it has the effect of being a "thermal onlooker." When magnetic fluid is applied to the tumor, the magnetic particles are diffusely and homogeneously acted upon by the alternative magnetic field, and the volume radiated gradually increases, killing tumor cells in the area containing the magnetic nanoparticles. Second, magnetic fluid heating is a nonactive material with high biological compatibility. Third, the therapeutic effect results from a physical conversion (ie, the alternative magnetic field generates heat). Fourth, the high temperature reached can increase the effects of chemotherapy and radiotherapy. The most recent studies[18] have shown that a constant temperature can be maintained automatically for thermotherapy by using ferromagnetic materials, based on the fact that these materials have magnetic properties and produce heat only when the temperature is lower than the Curie point. Once the temperature rises above the Curie point, they lose their magnetic properties and the temperature increase stops. This avoids any nonuniform uncontrolled temperature rise, which is important when thermotherapy is applied to the deeper layers of tumor tissue. Therefore, identification of a suitable magnetic induction material for magnetic fluid heating has become a hot topic in this area of research.[19]

A modified chemical coprecipitation method was initially used to prepare nanometric $Mn_xZn_{1-x}Fe_2O_4$ as a magnetic induction material for magnetic fluid heating to treat liver and cervical cancers, with satisfactory outcomes.[20,21] The ratio of Mn and Zn was adjusted to provide a specific Curie point.[22,23] This material is strongly magnetic when below the Curie point, absorbing electromagnetic waves from the alternative magnetic field, causing a temperature rise. When the temperature reaches the Curie point, the material becomes nonmagnetic and loses its ability to absorb electromagnetic waves, and the temperature decreases. When the temperature is below the Curie point, it recovers its magnetic properties and the temperature rises again. Temperature can now be controlled at a set Curie point, so the problems of lack of automatic temperature control and constant temperature in

thermotherapy are resolved, and the stability and safety of thermotherapy has improved. Biological compatibility and safety are important prerequisites in the clinical setting,[24] and studies of self-assembled Mn-Zn ferrite in this regard have had encouraging results.[25]

Binding of a receptor to its ligand is characterized by specificity, selectivity, saturation, strong affinity, and obvious biological effects. So far, one of the most active fields of study is the use ligands as carriers of drugs or radionuclides for targeted treatment, ie, increasing local drug concentrations in lesions via conductivity of the receptor in media, and improving the therapeutic effect while reducing toxicity. With better understanding of the folic acid receptor, it has been found that the activity and quantity of folic acid receptors on the membrane surface of various tumor cells (including ovarian, colorectal, breast, lung, and renal) is significantly higher than that of normal cells, which has laid the foundations for investigating folic acid as a targeted treatment for cancer.[26] Albumin contains abundant lysines, which account for about 10% of its total number of amino acids. Exposed lysine ε-amino and terminal amino groups on the surface of albumin nanoparticles (surface-reactive amino groups) are targets for effective chemical modification. For this reason, human serum albumin (HSA) nanoparticles have been coupled with the active ester of folic acid, used to target these surface-reactive amino groups, and their efficacy explored under different conditions. The rationale of this research was to exploit the high folic acid receptor expression on the surface of various tumor cells, thereby enabling targeted and enhanced uptake of albumin nanoparticles by tumor tissue.[27] After optimization of the experimental conditions, it was clearly seen on dextran gel column chromatography that folic acid-coupled albumin nanoparticles were totally separated from the active ester of folic acid, and the hydrolysate of trypsin in a mechanical mixture of folic acid coupled-albumin nanoparticles showed an ultraviolet absorption peak at 358 nm, demonstrating that folic acid had successfully coupled onto the surface of the albumin nanoparticles.

Because albumin nanoparticles are excellent carriers of radioactive nuclides, temperature can be used to enhance the efficiency of the rays, and synergism of various therapeutic methods is a trend in tumor treatment. The present study used [188]Re to achieve the triple-killing effect of targeted thermotherapy, chemotherapy, and radiotherapy.

Compared with related studies in China and other countries, our study was unique in using albumin nanoparticles as the carrier, the folic acid receptor as the target, and combining

chemotherapy, thermotherapy, and radionuclide therapy. It has solved not only the problems of automatic temperature control, but also combined the orientated killing effect of chemotherapy and nuclear radiation. This technique meets the requirements of safety, effectiveness, and specificity which are critical for any new biotherapeutic method being applied in the clinical setting.

Materials and methods
Instrumentation

The instruments used were a ^{188}W/^{188}Re generator (Shanghai Kexin Company, Shanghai, China), JA1003 electronic balance (Shanghai Balance Instrument Factory, Shanghai, China), GC911 gamma radioimmune counter (Zhongjia Photoelectric Instrument Branch Company General Company of Scitech Industry, China Scitech University, Zhejiang, China), GF-1 high speed disperser (Jiangsu Haimen Qilin Medical Instrument Factory, Jiangsu, China), DMC-1 direct current constant speed mixer (Shanghai Sile Instrument Factory, Shanghai, China), 34-061 activity meter (Victoreen Company, Cleveland, OH).

Pharmaceuticals and reagents

Human serum albumin (Shanghai Shenggong Biotech Company Ltd, Shanghai, China), $SnC1_2 \cdot 2H_2O$, sodium gluconate, acetic acid, acetate sodium, absolute alcohol, hydrochloric acid, and sodium hydroxide are all obtained as analytical pure reagents.

Preparation of ^{188}Re-folate-CDDP/HSA magnetic nanoparticles

^{188}ReO$_4^-$ cleansing solution was obtained using a ^{88}W/^{188}Re generator (Shanghai Kexin Company) and was used directly for labeling without purification. The labeling process was as follows: 0.1 mL sodium gluconate solution (0.3 mol/L), 0.1 mL stannous chloride dissolved in strong hydrochloric acid (10 mg/mL), 0.04 mL acetic acid buffer solution (pH 5.0, 0.2 mol/L), and 30 mg folate-CDDP/HSA magnetic nanoparticles in a centrifuge tube.[27] The mixture was then shaken and kept at room temperature for one hour. A 0.1 mL sample of ^{188}ReO$_4^-$ cleansing solution was added and shaken for five hours at room temperature to complete the labeling.

Determination of labeling rate

A thin-layer hierarchical analytic procedure was used. A GF254 silica gel plate was selected as the supporting material and baked at 56°C in an air oven for 30 minutes before use. The silica gel plate was cut into 0.5 cm × 10 cm pieces

and a primary point was marked with a pencil 1 cm away from the bottom edge of the test paper. Ten lateral equidistant lines were drawn with a pencil, and 10 checks were reserved for use. A test tube was taken and checked, and a developing agent was added, comprising alcohol:ammonia:water (2:1:5 v/v). A capillary tube was used to suction the labeled ^{188}Re-folate-CDDP/HSA magnetic nanoparticles from an Eppendorf tube, which were dropped at the primary point, dried, and then analyzed using the hierarchical analytic procedure. The analytic paper was taken out, dried, cut into 10 pieces as per the drawn checks, and the pieces were put into a polyethylene test tube to determine radioactivity (radiofrequency was 0 for the gel labeled with ^{188}Re and 0.7–0.8 for the ^{188}Re-folate-CDDP/HSA magnetic nanoparticles and ^{188}ReO$_4^-$). The radioactive distribution for each analytic paper was determined, and the labeling rate was measured using the following formulae:

Radiofrequency = Distance between component to be tested and primary point/distance between frontal mobile phase and primary point

Labeling rate (%) = Sum of radioactive counting rate of labeled material/total radioactive counting rate × 100%.

Determination of the radiochemical purity of the ^{188}Re-folate-CDDP/HSA magnetic nanoparticles was done using the following methods.

Optimization of labeling conditions for ^{188}Re-folate-CDDP/HSA nanoparticles

The relationship between the various parameters and labeling rate was investigated by determination of labeling rate when changing one parameter of the labeling conditions while leaving the other parameters unchanged. Labeling rates were determined under different conditions to obtain optimum labeling:

- Radiochemical purity at 1, 2, 3, 4, 5 and 6 hours after labeling
- pH value of the acetic acid buffer solution 4.0–6.0
- Volume of cleansing solution 50–200 μL
- Volume of stannous chloride 50–1500 μg
- Labeling material reacted at room temperature or in a 37°C water bath for 5 hours.

In vitro stability of ^{188}Re-folate-CDDP/HSA nanoparticles

The labeled magnetic nanoparticles were washed twice with distilled water and normal saline, and were then dispersed in 1 mL of calf serum, oscillated and incubated at 37°C, with

sampling at 0, 2, 4, 8, 12, 24, 48 and 72 hours. Radioactive counting was then performed.

Experimental animals

Twenty-one female BALB/C nude mice, aged 4 weeks and weighing 15–19 g, were obtained from the Experimental Animal Center at Jiangsu Institute of Nuclear Medicine.

Tumor cell culture

Human ovarian cancer SKOV3 cells were supplied by the Shanghai China Typical Cell Culture Collection Center. Routine culture and generation of next-generation human ovarian cancer SKOV3 cells were carried out in 5% CO_2 and at 37°C in an air oven with calf serum 10%, penicillin 100 U/mL, streptomycin 100 mg/mL, insulin 40 U, and McCoy's 5A culture medium with a pH of 7.4.

Tumor-bearing nude mouse model

Human ovarian cancer SKOV3 cells were implanted under the skin on the right side in 21 BALB/C nude mice. The inoculation volume was 0.1 mL (concentration of living cells 1×10^7/mL). After inoculation, tumor nodes appeared at the inoculated site, which were observed continuously for 2 weeks. Tumors were judged to have formed from the appearance of hard tumor nodes at the inoculated site and increasing nodal enlargement. The mice were raised in an appropriate animal house, and fed with cool boiled water and fodder sterilized with steam. The wood chips used for bedding were sterilized with steam, and the mouse cages were sterilized with a disinfectant solution. Water, fodder, wood chips, and cages were changed and cleaned once a day, ambient temperature was kept at 22°C ± 1°C and humidity at 60% ± 10%, on a 12-hour day/night cycle. Maximum tumor diameter was measured using a vernier caliper.

Biodistribution of ^{188}Re-folate-CDDP/HSA magnetic nanoparticles

All animal experiments were carried out in compliance with national laws relating to animal research. The 21 BALB/C tumor-bearing nude mice were randomized into seven groups, with three mice in each group. ^{188}Re-folate-CDDP/HSA magnetic nanoparticles (0.74 MBq/0.2 mL) were injected into the tail veins of the mice in each group. The mice were then sacrificed by cervical dislocation at 0.5, 1, 2, 4, 8, 24, and 48 hours after injection. Blood, brain, heart, liver, spleen, lung, kidney, stomach, small intestine, muscle, ovary, pancreas, gall bladder, and tumor were removed for measurement of weight,

radioactivity count, and percentage of injected volume per gram (% ID/G) after radioactive decay was calculated.

Statistical analysis

SPSS version 3.0 (SPSS Inc, Chicago, IL) was used for *t*-testing and single-factor analysis of variance. Numerical data were expressed as the mean ± standard deviation. A *P* value <0.05 was considered to be statistically significant.

Results

Influence of reaction time on radiochemical purity

Changes in radiochemical purity were measured at 1, 2, 3, 4, 5 and 6 hours after labeling, and the results are shown in Figure 1. Radiochemical purity increased with prolonging of the reaction time and reached 92.39% ± 3.86% after 5 hours versus 78.67% ± 5.57% after 4 hours. This difference was statistically significant (n = 3, $0.01 < P < 0.05$).

Influence of pH buffer solution on radiochemical purity

When other conditions were kept constant and the pH of the buffer solution was changed, radiochemical purity > 85% was achieved when the pH was 4.0–5.5, and was 94.6% ± 2.67% when the pH was 5.0. This difference was statistically significant (n = 3, $P < 0.01$) compared with 75.4% ± 3.56% when pH was 6.0. The results are shown in Figure 2.

Influence of cleansing solution volume on radiochemical purity

When other conditions were kept constant and the cleansing solution volume was changed, radiochemical purity was >85% when the volume was 100–200 µL and 75.8% ± 4.93% when the volume was 250 µL
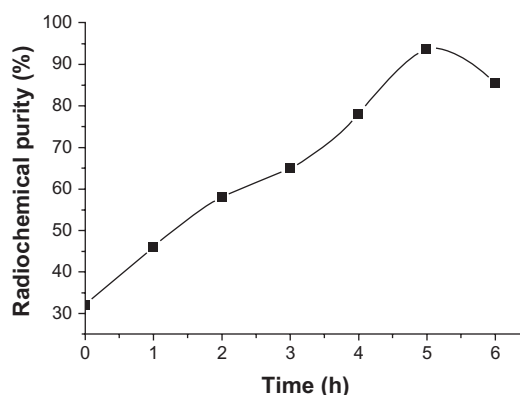

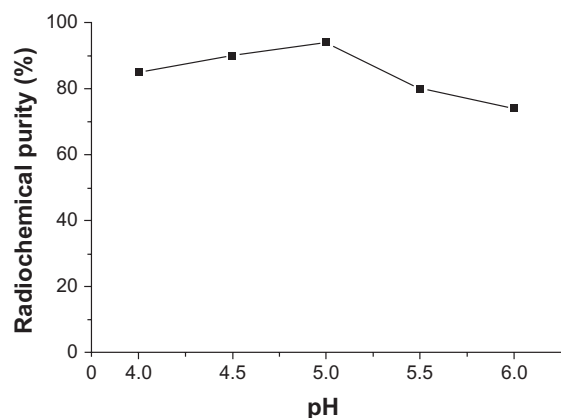**Figure 1** Influence of reaction time on radiochemical purity.

Figure 2 Influence of pH of buffer solution on radiochemical purity.

Figure 4 Influence of SnC$I_2 \cdot 2H_2O$ concentration on radiochemical purity.

(Figure 3). This difference was statistically significant (n = 3, 0.01 < P < 0.05) compared with a radiochemical purity of 92.7% + 5.19% when the volume was 150 µL.

Influence of SnCl$_2 \cdot 2H_2O$ use on radiochemical purity

When other conditions were kept constant and the concentrations of SnCl$_2 \cdot 2H_2O$ were changed, radiochemical purity >90% was obtained with a higher volume of SnCl$_2 \cdot 2H_2O$ (>1000 µg, see Figure 4). Radiochemical purity was <70% at 500 µg of SnCl$_2 \cdot 2H_2O$, and was 61.46% ± 3.56% and 92.51% ± 4.72% at 500 µg and 1000 µg of SnCl$_2 \cdot 2H_2O$, respectively. This difference was statistically significant (n = 3, P < 0.01). The gel content was lower than 10% in all labeled reactions.

Influence of reaction temperature on radiochemical purity

The effect of reaction temperature was compared between room temperature and a 37°C water bath for 5 hours,
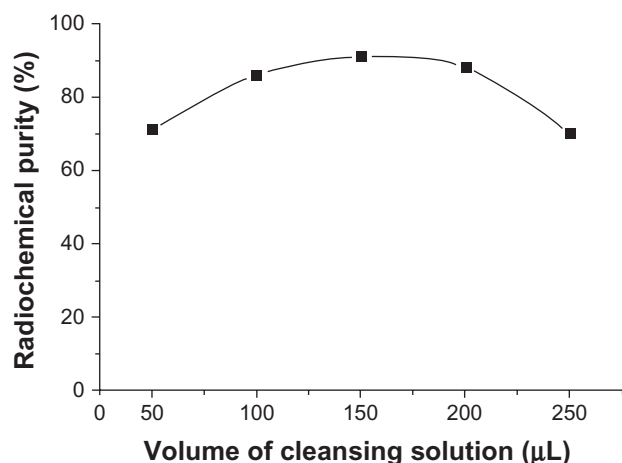
giving a radiochemical purity of 95.78% ± 1.61% and 95.96% ± 1.32%, respectively. The difference was not statistically significant (n = 3, P > 0.05).

In vitro stability

Radiochemical purity of [188]Re-folate-CDDP/HSA magnetic nanoparticles in calf serum was 95.57% ± 0.09% at 37°C, and values were stable over 2, 4, 8, 12, 24, 48, and 72 hours, being 95.29% ± 1.00%, 94.65% ± 0.78%, 91.26% ± 0.99%, 88.53% ± 0.91%, 85.2% ± 0.7%, 83.38% ± 0.22%, and 80.30% ± 0.11%, respectively (Figure 5).

Tumor growth in nude mice

Two weeks after inoculation with the tumor cells, nodes appeared under the skin at the inoculated site. These grew larger, were round or oval, protruded above the skin surface, and the skin on the tumor surface became thinner, semitransparent, and smooth. After 3 weeks, the tumor diameter was about 0.5 cm.
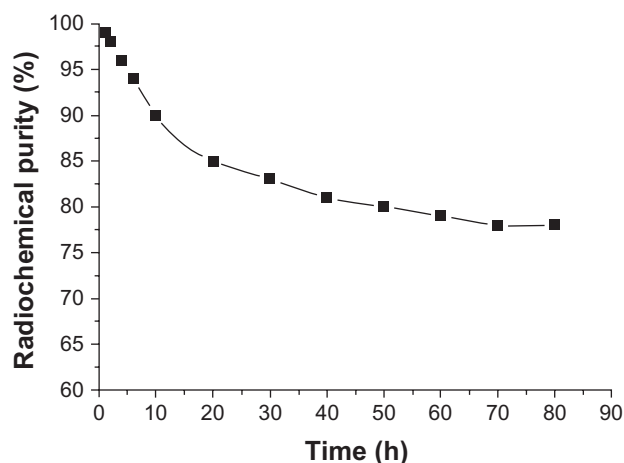

Figure 3 Influence of cleansing solution volume on radiochemical purity.

Figure 5 Stability of [188]Re-folate-CDDP/HSA magnetic nanoparticles in calf serum.

Biodistribution of ^{188}Re-folate-CDDP/HSA magnetic nanoparticles

The distribution of ^{188}Re-folate-CDDP/HSA magnetic nanoparticles in the organs and tumor tissues of the tumor-bearing nude mice is shown in Table 1. It can be seen that the ^{188}Re-folate-CDDP/HSA magnetic nanoparticles injected via the tail vein were distributed mainly in the liver, kidney, stomach, intestine, and tumor tissue. The radioactivity in blood decreased rapidly after injection, and in vivo radioactivity was not detectable after 24 hours. Radioactivity of the tumor tissues reached a peak value of 7.86% ± 0.91% ID/g at 8 hours, at which time the radioactive ratio of tumor to opposite muscle also reached a maximum of 8.83 ± 1.71.

Discussion

Radiotherapy destroys or injures tumor cells by introducing radioactive nuclides into the tumor. The radioactive nuclides used include alpha or beta particles, Auger electrons, and internal conversion electrons. ^{188}Re, obtained by a ^{188}W/^{188}Re generator, has excellent nuclear properties, with a physical half-life of 16.9 hours.[28] It mainly transmits beta-rays for tumor treatment, with a ray energy of 2.11 MeV (79%) and 1.97 MeV (20%). It also transmits 155 keV gamma rays suitable for imaging. A radioactive detector outside the body can be used for tracing and imaging. ^{188}Re and its labeled compound have clear therapeutic effects in tumor tissue, synovial membranes in the joints, and postoperative arterial stenosis, with minor side effects. With a high linear density of energy transmission, it can also kill distant tumor cells and tumor cells at the nonproliferation stage where chemotherapy fails, so is widely used as a component in radioactive agents.[29]

Direct labeling or chelatometry can be used to label ^{188}Re on HSA. Chelatometry uses a dual-function chelant to connect ^{188}Re with amino acids in a protein molecule. The chelant should be linked to the protein molecule before labeling. Direct labeling methods include the pre-tin method and the stepwise reduction method. This study used the pre-tin method for direct labeling of ^{188}Re on HSA. There are several possible explanations for this labeling method.[23] First, the reducing agent ($SnCl_2$) opens the bisulfur bond on the protein molecule, exposing the sulfhydryl group of cysteine in the protein, which combines with $SnCl_2$ to form a compound. Second, the valence state of ^{188}Re is reduced by $SnCl_2$ and a medium ligand forms the chelate. Third, ^{188}Re in the chelate is displaced to the sulfhydryl group of cysteine in the protein molecule.

The electrode potential of ^{188}ReO$_4^-$ is relatively low and difficult to reduce. While it is helpful to reduce ^{188}ReO$_4^-$, a high concentration of $SnCl_2$ is easy to react with Re in the system to form Re-Sn gel. Rhodes reported[30] that about 4% of the bisulfur bonds in the protein molecule are reduced. During reduction, only the outer bisulfur bonds should be reduced, and not involve the main bisulfur bonds which maintain the structural integrity of the protein molecule. Using acetic acid buffer solution to adjust the pH of the reaction system is easier than using sodium hydroxide. When the pH is lower than 4.0, it will affect the bioactivity of the label. ^{188}Re (V) will reoxidize to ^{188}ReO$_4^-$ when the pH is higher than 5.5. When the pH is 4.5–5.0, it can prevent formation of insoluble oxides of tin and Re.[25] When the cleansing

Table 1 Biodistribution of ^{188}Re-folate-CDDP/HSA magnetic nanoparticles in mice with a gamma counter

Organ	Time after injection (hours)						
	0.5	1	2	4	8	24	48
Blood	2.41 ± 0.75	1.70 ± 0.36	1.92 ± 0.51	1.94 ± 0.32	2.83 ± 2.15	0.38 ± 0.16	0.30 ± 0.17
Brain	0.19 ± 0.04	0.10 ± 0.02	0.09 ± 0.04	0.09 ± 0.03	0.08 ± 0.04	0.05 ± 0.01	0.03 ± 0.01
Heart	0.98 ± 0.43	1.55 ± 0.46	0.68 ± 0.21	0.72 ± 0.13	0.49 ± 0.17	0.09 ± 0.03	0.14 ± 0.01
Liver	4.48 ± 1.93	2.18 ± 0.91	1.67 ± 1.20	2.17 ± 0.83	1.65 ± 0.41	0.69 ± 0.15	0.55 ± 0.03
Spleen	2.68 ± 1.05	1.88 ± 0.52	1.66 ± 0.43	1.39 ± 0.34	2.68 ± 0.61	0.58 ± 0.13	0.38 ± 0.02
Lung	2.07 ± 0.81	1.59 ± 0.37	1.88 ± 0.61	1.68 ± 0.38	0.99 ± 0.47	0.48 ± 0.23	0.43 ± 0.22
Kidney	2.19 ± 0.40	1.28 ± 0.17	1.45 ± 0.29	1.37 ± 0.30	0.87 ± 0.32	0.16 ± 0.03	0.15 ± 0.01
Stomach	5.78 ± 3.50	3.76 ± 1.51	7.49 ± 1.20	9.59 ± 1.93	5.81 ± 2.38	0.27 ± 0.03	0.15 ± 0.03
Small intestine	2.28 ± 0.51	2.09 ± 0.61	2.88 ± 1.03	3.08 ± 1.31	1.99 ± 1.44	0.18 ± 0.10	0.12 ± 0.02
Contralateral muscle	0.55 ± 0.33	0.48 ± 0.05	1.11 ± 0.73	0.58 ± 0.10	0.89 ± 0.43	0.14 ± 0.03	0.16 ± 0.03
Ovaries	1.27 ± 0.38	0.49 ± 0.07	0.88 ± 0.45	0.79 ± 0.13	0.68 ± 0.27	0.16 ± 0.09	0.19 ± 0.16
Pancreas	1.25 ± 0.52	0.59 ± 0.20	0.98 ± 0.48	1.36 ± 0.33	0.69 ± 0.26	0.15 ± 0.04	0.09 ± 0.01
Bladder	1.95 ± 0.22	0.89 ± 0.61	1.39 ± 0.78	2.35 ± 1.12	1.85 ± 1.42	0.49 ± 0.27	0.33 ± 0.02
Tumor	2.15 ± 1.43	2.18 ± 0.57	2.58 ± 0.23	3.44 ± 0.45	7.86 ± 0.91	0.79 ± 0.24	0.20 ± 0.01

Notes: Values are expressed as % ID/g (percent of injected dose per gram tissue). Data are presented as the mean ± standard deviation.

solution volume is small, the radiochemical purity increases with an increasing volume of cleansing solution, but when the cleansing solution volume increases beyond a certain level, the concentrations of [188]Re and the labeled substrate in the reaction system decrease correspondingly, resulting in decreased radiochemical purity. Radiochemical purity at an ambient temperature of 22°C or in a 37°C water bath was not significantly different. Because labeling of the polypeptide at ambient temperature is ideal, a temperature of 22°C was selected for labeling. In this study, the labeling rate for the prepared [188]Re-folate-CDDP/HSA magnetic nanoparticles was over 90%, and their radiochemical purity was over 95%. Labeling done in calf serum at 37°C yielded a labeling rate of 83% at 72 hours, which is suitable for clinical use. The [188]Re-folate-CDDP/HSA magnetic nanoparticles was then injected into tumor-bearing nude mice through the tail vein. Because the activity and quantity of folic acid receptors on the surface of the ovarian cancer cell membrane is significantly higher than that on normal cells, folic acid coupled to the albumin surface of the nanoparticles binds specifically with the folic acid receptor on the surface of the ovarian cancer cell membrane. Meanwhile, the radionuclide on the carrier acts on tumor cells specifically, playing a targeting role, resides in tumor cells for a long time, delivering a higher radiation dose to the tumor tissue. These nanoparticles can also kill or injure tumor cells around the target area, and in this way, the tumor-suppressing effect is increased.

In the present study, after the [188]Re-folate-CDDP/HSA magnetic nanoparticles were injected into tumor-bearing nude mice, they were widely distributed in different tissues and organs, and the tissue concentration and distribution decreased with time. [188]Re-folate-CDDP/HSA magnetic nanoparticles were taken up in significant amounts by the stomach, followed by the liver and small intestine. Compared with the liver, the concentration in the kidney was less, indicating that [188]Re-folate-CDDP/HSA magnetic nanoparticles may be less toxic to the liver, helping to mitigate hepatic metabolism of cancer chemotherapy and the burden on the kidney. Our results indicate that [188]Re-folate-CDDP/HSA magnetic nanoparticles underwent predominantly digestive metabolism after injection into mice. A significant amount of radioactivity was cleared from the body by 24 hours, but further study of clearance is needed. Tumoral uptake of [188]Re-folate-CDDP/HSA magnetic nanoparticles reached a peak at 8 hours of 7.86 ± 0.91 (% ID/g), the ratio of tumor/muscle increased gradually after injection, reaching a maximum of 8.83 ± 1.71 at 8 hours, then decreased gradually, and radioactivity in vivo appeared to be eliminated at 24 hours.

It is suggested that [188]Re-folate-CDDP/HSA magnetic nanoparticles could be used as radionuclide targeted treatment for tumors.

Our results also suggest that [188]Re-folate-CDDP/HSA magnetic nanoparticles are distributed in nontarget organs and for a longer duration by intravenous administration, which may result in radioactive organ damage, especially in the liver, kidney, and gastrointestinal tract, and this may be an important issue in the targeted radionuclide treatment of cancer. The issue is expected to be resolved by using appropriate methods to reduce the normal organ uptake of radionuclides and to speed up their metabolism. Ingestion of a fatty meal can limit the excessive uptake of [188]Re-folate-CDDP/HSA magnetic nanoparticles in the stomach. Percutaneous intratumoral injection of [188]Re-folate-CDDP/HSA magnetic nanoparticles may also be a useful method by which to reduce radiation damage to normal tissues and organs, enabling the radionuclides to remain in the tumor tissue, and also plays a role as a tumor marker. Direct percutaneous intratumoral injection in solid tumors is a promising route of administration and requires further research in the future.

Acknowledgment

Disclosure

The authors report no conflicts of interest in this work.

References

1. McGuire WP, Hoskins WJ, Brady MF, et al. Cyclophosphamide and cisplatin compared with paclitaxel and cisplatin in patients with stage III and stage IV ovarian cancer. *N Engl J Med*. 1996;334(1):1–6.
2. Zhao Z, Li H, Wu M, Zhan J. Temperature autocontrol and stabilization in the thermotherapy of tumors. *Progress in Biochemistry and Biophysics*. 1997;24(6):504–506.
3. Eveno C, Dagois S, Guillot E, Gornet JM, Pocard M. Treatment of peritoneal carcinomatosis with surgery and hyperthermic peroperative intraperitoneal chemotherapy (HIPEC): new aspects and validated indications. *Bull Cancer*. 2008;95(1):141–145.
4. McQuellon RP, Russell GB, Shen P, Stewart JH 4th, Saunders W, Levine EA. Survival and health outcomes after cytoreductive surgery with intraperitoneal hyperthermic chemotherapy for disseminated peritoneal cancer of appendiceal origin. *Ann Surg Oncol*. 2008;15(1):125–133.
5. Gesson-Paute A, Ferron G, Thomas F, de Lara EC, Chatelut E, Querleu D. Pharmacokinetics of oxaliplatin during open versus laparoscopically assisted heated intraoperative intraperitoneal chemotherapy (HIPEC): an experimental study. *Ann Surg Oncol*. 2008;15(1):339–344.

6. Armstrong DK, Bundy B, Wenzel L, et al. Gynecologic Oncology Group. Intraperitoneal cisplatin and paclitaxel in ovarian cancer. *N Engl J Med*. 2006;354(1):34–43.

7. Shen P, Levine EA, Hall J, et al. Factors predicting survival after intraperitoneal hyperthermic chemotherapy with mitomycin C after cytoreductive surgery for patients with peritoneal carcinomatosis. *Arch Surg*. 2003;138(1):26–33.

8. Pestieau SR, Marchettini P, Stuart OA, Chang D, Sugarbaker PH. Prevention of intraperitoneal adhesions by intraperitoneal lavage and intraperitoneal 5-fluorouracil: experimental studies. *Int Surg*. 2002;87(3):195–200.

9. Yoshida Y, Sasaki H, Kurokawa T, et al. Efficacy of intraperitoneal continuous hyperthermic chemotherapy as consolidation therapy in patients with advanced epithelial ovarian cancer: a long-term follow-up. *Oncol Rep*. 2005;13(1):121–125.

10. Gori J, Castaño R, Toziano M, et al. Intraperitoneal hyperthermic chemotherapy in ovarian cancer. *Int J Gynecol Cancer*. 2005; 15(2):233–239.

11. Gilchrist RK, Medal R, Shorey WD, Hanselman RC, Parrott JC, Taylor CB. Selective inductive heating of lymph nodes. *Annals of Oncology*. 1957;146(4):596–606.

12. Jordan A, Scholz R, Wust P, et al. Effects of magnetic fluid hyperthermia (MFH) on C3H mammary carcinoma in vivo. *Int J Hyperthermia*. 1997;13(6):587–605.

13. Jordan A, Wust P, Scholz R, et al. Cellular uptake of magnetic fluid particles and their effects on human adenocarcinoma cells exposed to AC magnetic fields in vitro. *Int J Hyperthermia*. 1996;12(6):705–722.

14. Kotte AN, van Wieringen N, Lagendijk JJ. Modelling tissue heating with ferromagnetic seeds. *Phys Med Biol*. 1998;43(1):105–120.

15. Yan S, Zhang D, Gu N, et al. Therapeutic effect of Fe_2O_3 nanoparticles combined with magnetic fluid hyperthermia on the cultured human liver cancer cells and xenograft liver cancers. *J Nanosci Nanotechnol*. 2005;5(8):1185–1192.

16. Zhang D, Tang Q, Wang Z, Fan X. Therapeutic effects of nano-magnetoliposomes containing As_2O_3 combined with magnetic fluid hyperthermia on xenograft cervical carcinoma. *Chinese J Phys Med Rehabil*. 2006;26(2):102–104.

17. Brezovich IA, Lilly MB, Meredith RF, et al. Hyperthermia of pet animal tumours with self-regulating ferromagnetic thermoseeds. *Int J Hyperthermia*. 1990;6(1):117–130.

18. Ajay K, Gupta M. Synthesis and surface engineering of iron oxide nanoparticles for biomedical applications. *Biomaterials*. 2005; 26(18):3995–4021.

19. Cong X, Zhang D, Tang Q, Gu N, Zhao S, Zhang J. Biocompatibility of $Mn0.5Zn0.5Fe_2O_4$ nanoparticles used in tumor hyperthermia. *Journal of Southeast University (Natural Science Edition)*. 2007;37(3):216–219.

20. Sudimack J, Lee RJ. Targeted drug delivery via the folate receptor. *Adv Drug Deliv Rev*. 2000;41(2):147–162.

21. Xiang J, Xue W, Xiao J, et al. The preparation of folate-conjugated human serum albumin (folate-HSA). *China Medical Herald*. 2009;6(28):15–16.

22. Olson P, Callins VP, Liu L. Internalisation and retention of EGF-dextran associated radioactivity in transfected Chinese hamster ovary cells expressing the human EGF-receptor. *Int J Oncol*. 2002;20(5):1057–1063.

23. Dadachovs E, Mirzadeh S. The role of tin in the direct labelling of proteins with Rhenium-188. *Nucl Med Biol*. 1997;24(6):605–608.

24. Chen WJ, Yen CL, Lo ST, Chen KT, Lo JM. Direct 99m Tc labeling of Herceptin (trastuzumab) by 99m Tc(I) tricarbonyl ion. *Appl Radiat Isot*. 2008;66(3):340–345.

25. Iznaga-Escobar N. Direct radiolabeling of monoclonal antibodies with rhenium-188 for radioimmunotherapy of solid tumors – a review of radiolabeling characteristics, quality control and in vitro stability studies. *Appl Radiat Isot*. 2001;54(3):399–406.

26. Chen D, Tang Q, Xue W, Wang X. The feasibility of using magnetic nanoparticles modified as gene vector. *West Indian Med J*. 2010;59(3):300–305.

27. Liu H, Zhu L. Study on preparation and targetibility of folate receptor-mediated antitumor nanoparticles entrapping arsenic trioxide. *Lishizhen Medicine and Material Medica Research*. 2008;19(3):666–667.

28. Yin DZ, Hu WQ, Cai XM, et al. A study on preparation of W2 Re Generator. *Nucltech*. 1998;21(1):51–55.

29. Knapp FF, Beets AL, Guhllke S, et al. Availability of rhenium-188 from the alumina-based tungsten-188/rhenium-188 generator for preparation of rhenium-188-labeled radiopharmaceuticals for cancer treatment. *Anticancer Res*. 1997;17(3B):1783–1795.

30. Rhodes BA. Direct labeling of proteins with 99m-Tc. *Nucl Med Biol*. 1991;18(7):667–676.